

Echo-Planar Diffusion-Tensor Imaging of Inner Field-of-Views in the Human Brain and Spinal Cord Using 2D-Selective RF Excitations

J. Finsterbusch^{1,2}

¹Dept. of Systems Neuroscience, University Medical Center Hamburg-Eppendorf, Hamburg, Germany, ²Neuroimage Nord, Hamburg-Kiel-Lübeck, Germany

Introduction

Echo-planar imaging (EPI) [1] suffers from geometric distortions in the presence of magnetic field inhomogeneities which hamper its applicability, in particular at high static magnetic fields. Because these artifacts depend on the field-of-view (FOV) in the phase-encoding direction, several approaches to acquire inner field-of-views without aliasing have been presented in the past, e.g. using cross-sectional RF excitations [2,3] or spatially two-dimensional selective RF (2DRF) excitations [4–6]. In this work, the feasibility of EPI with 2DRF excitations for diffusion-tensor imaging (DTI) of inner field-of-views in the human brain and cervical spinal cord at high in-plane resolutions is demonstrated.

Methods

2DRF excitations were implemented based on a fly-back blipped-planar trajectory. The blip direction of the 2DRF trajectory was chosen to coincide with the phase encoding direction of the EPI trajectory, the line direction of the 2DRF was along the slice-selection direction (Fig. 1a). In this setup, the unwanted, periodic side excitations appear in phase-encoding direction and were positioned outside of the object (Fig. 1b). Measurements were performed on a 3T whole-body MR system (Siemens Magnetom Trio) using a twelve-channel head coil or a four channel neck coil for signal reception. In-plane resolutions of $0.9 \times 0.9 \text{ mm}^2$ and $0.5 \times 0.5 \text{ mm}^2$ were investigated at a slice thickness of 5 mm. A $5 \times 45 \text{ mm}^2$ rectangular profile was defined for the 2DRF and realized with 19 k-space lines using a resolution of $5 \times 10 \text{ mm}^2$ and a field-of-excitation of 190 mm which was chosen to shift the unwanted side excitations outside of the object. The field-of-view covered 36 mm in phase encoding direction, i.e. the plateau of the excitation profile, plus 14 mm oversampling to omit the transition regions from the field-of-view (see Fig. 1b). Diffusion weighting was applied in six non-collinear directions with b values of 750 s mm^2 (for $0.9 \times 0.9 \text{ mm}^2$) or 625 s mm^2 (for $0.5 \times 0.5 \text{ mm}^2$). 24 magnitude averages were performed within a total acquisition time of 12.6 min. Maps of the fractional anisotropy (FA), colour-coded with the principal diffusion direction (z-component in blue, y-component in green, x-component in red), were calculated by an algorithm provided by the manufacturer. For anatomical reference images, single-echo or multi-echo FLASH acquisitions were performed with a resolution of $0.5 \times 0.5 \times 5 \text{ mm}^3$.

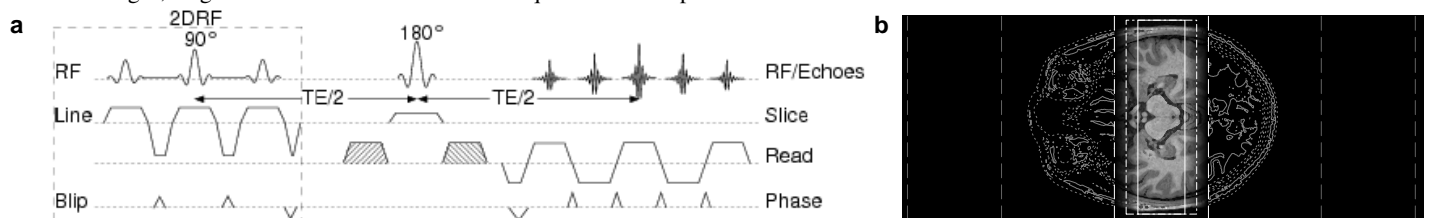


Figure 1: (a) Basic pulse sequence used in the present study and (b) schematic depiction of the FOV (solid) including oversampling (dash-dotted) and the areas excited by the 2DRF (dashed) including the side excitations (gray). For details see text.

Results and Discussion

A comparison of the non-diffusion-weighted images obtained with inner-FOV EPI in the human brain to standard slice-selective EPI is shown in Figure 2. The improved resolution reveals finer details and also reduces ringing artifacts from CSF. Colour-coded maps of the fractional anisotropy acquired in the cerebellum and the cervical spinal cord are shown in Fig. 3 in comparison with anatomical reference images. In the cerebellum, the major branches of the *arbor vitae* can be identified (arrows) and show the expected fibre orientation. In the spinal cord, the gray matter can be identified on the sagittal (Fig. 3b, arrows) and transverse (Fig. 3c) sections showing reduced anisotropy values compared to the surrounding white matter.



Figure 2: Non-diffusion-weighted images acquired (a) with standard slice-selective EPI ($2 \times 2 \times 5 \text{ mm}^3$ resolution) and (b) inner-FOV EPI with resolutions of (b) $0.9 \times 0.9 \times 5 \text{ mm}^3$ and (c) $0.5 \times 0.5 \times 5 \text{ mm}^3$.

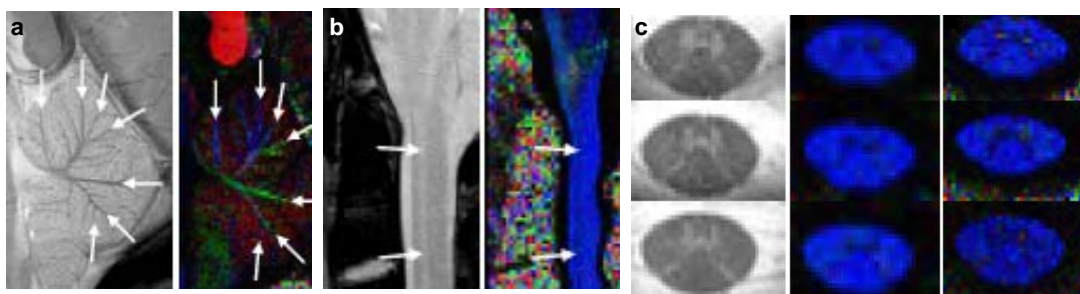


Figure 3: Colour-coded FA maps (right) and anatomical reference images (left) in (a) the cerebellum and (b,c) the cervical spinal. The right column in (c) is based on an in-plane resolution of $0.5 \times 0.5 \text{ mm}^2$, the other FA maps on $0.9 \times 0.9 \text{ mm}^2$.

References

- [1] Mansfield P, *J. Phys. C* **10**, 349–352 (1977)
- [2] Wheeler-Kingshott CA *et al.*, *Magn. Reson. Med.* **47**, 24–31 (2002)
- [3] Jeong EK *et al.*, *Magn. Reson. Med.* **54**, 1575–1579 (2005)
- [4] Bottomley PA, Hardy CJ, *J. Appl. Phys.* **62**, 4284–4290 (1987)
- [5] Rieseberg S *et al.*, *Magn. Reson. Med.* **47**, 1186–1193 (2002)
- [6] Saritas EU *et al.*, *Magn. Reson. Med.* **60**, 468–473 (2008)